Close-packing transitions in clusters of Lennard-Jones spheres

Florent Calvo, Mohammed Benali, Vincent Gerbaud, Mehrdji Hemati

Close-packing transitions in clusters of Lennard-Jones spheres

F. Calvo
Laboratoire de Physique Quantique, IRSAMC, Université Paul Sabatier, 118 Route de Narbonne, F31062 Toulouse Cedex, France

M. Benali and V. Gerbaud
Laboratoire de Génie Chimique, UMR 5503, BP 1301, 5 rue Paulin Talabot 31106 Toulouse Cedex, FRANCE

The structures of clusters of spherical and homogeneous particles are investigated using a combination of global optimization methods. The pairwise potential between particles is integrated exactly from elementary Lennard-Jones interactions, and the use of reduced units allows us to get insight into the effects of the particle diameter. As the diameter increases, the potential becomes very sharp, and the cluster structure generally changes from icosahedral (small radius) to close-packed cubic (large radius), possibly through intermediate decahedral shapes. The results are interpreted in terms of the effective range of the potential.

PACS numbers:

I. INTRODUCTION

Atomic and molecular clusters display very rich structural properties [1–3]. Due to their large surface/volume ratio, these finite systems often show symmetry elements that are not observed in bulk matter. For instance, fivefold and icosahedral geometries, while being forbidden in periodic systems, are ubiquitous in clusters ranging from rare-gas [4] to simple metals [5]. Clusters of molecules also display such pentagonal elements, even though the appearance of the bulk crystalline features usually occurs at smaller sizes with respect to atomic systems. In general, the icosahedral structure remains the most stable at small sizes, and more compact shapes become favored above some crossover size. The transition takes place near 1500 atoms for argon [4], near 200 molecules for N_2 [6], and only 30 for CO_2 [7]. The preference of larger molecules toward close-packed structures has been confirmed in the $(C_{60})_n$ system [8].

The interaction between larger structures is usually harder to consider because of the internal degrees of freedom. Several studies have emphasized the possible rearrangements during the soft collision between clusters [9, 10]. Thanks to their outer ligand layer, colloidal particles are less sensitive to such isomerizations. However, unless the liquid suspension is removed they do not form superstructures. The interaction between colloidal particles, even with only a few hundred atoms, cannot be calculated exactly at the level of atomic details. Instead, coarse-grained approximations such as those introduced by Hamaker [11] provide the main features governing this interaction. In the present paper, we investigate clusters of spherical particles assumed to be homogeneously filled with Lennard-Jones (LJ) centers. By varying the radius of the particles from small to large values, we explore the transition from the atomic scale to the mesoscale, and its consequences on the shape of the nano-assemblies.

Finding the stable structures of a many-particle system, even bound by simple forces, can be very difficult because of the huge number of minima on the potential energy surface (PES) [12]. Powerful numerical algorithms have been dedicated to solve this task, especially the basin-hopping, or Monte Carlo+minimization algorithm of Wales and Doye [13]. Such an approach is useful in the case where the cluster contains relatively few particles (below about 100), but is not practical for large sizes, for which we will use extrapolations to the cohesion energies for the magic number series. The article is organized as follows. In the next section, we describe the interaction between particles and discuss them in terms of an effective range. Section III presents our results on the structure as a function of both the number of particles and the particles' radius. We finally summarize and conclude in Sec. IV.

II. METHODS

We consider spherical particles (1) and (2) with common radius R and constant volumic density ρ. The interaction between two elements of volume ρd^3r_1 and ρd^3r_2 distant by $r' = |\mathbf{r}_1 - \mathbf{r}_2|$ is assumed to be a Lennard-Jones form

$$d^6V = 4\varepsilon \left[\left(\frac{\sigma}{r'}\right)^{12} - \left(\frac{\sigma}{r'}\right)^{6} \right] \rho^2 d^3r_1 d^3r_2. \quad (1)$$

Both the repulsive and attractive parts can be integrated exactly: the result for a $1/r^n$ potential only depends on the distance d between the centers of mass of the two particles as

$$V^{(n)}(d) = -\frac{4\pi^2}{(n-2)(n-3)(n-4)(n-5)}\left[\frac{1}{n-6}\left(\frac{2}{d^{n-6}} - \frac{1}{(d+2R)^{n-6}} - \frac{1}{(d-2R)^{n-6}}\right)\right.$$
$$\left. -\frac{1}{D(n-7)}\left(\frac{2}{d^{n-7}} - \frac{1}{(d+2R)^{n-7}} - \frac{1}{(d-2R)^{n-7}}\right) + \frac{R^2}{d}\left(\frac{2}{d^{n-5}} + \frac{1}{(d+2R)^{n-5}} + \frac{1}{(d-2R)^{n-5}}\right)\right] \quad (2)$$

for $n > 6$, and

$$V^{(6)}(d) = -\frac{\pi^2}{2}\left[\ln\frac{(d+2R)(d-2R)}{d^2} + \frac{R^2}{d}\left(\frac{2}{d} + \frac{1}{d+2R} + \frac{1}{d-2R}\right)\right] \quad (3)$$

for $n = 6$ [11]. The resulting interaction between two identical spheres is proportional to ρ^2 and ε. Furthermore, if we assume that the LJ parameter σ fixes the scale of all distances, setting it to 1 leads to

$$V(d) = 4\varepsilon\rho^2\left[V^{(12)}(d) - V^{(6)}(d)\right]. \quad (4)$$

Due to the presence of many terms in the potential, there is no explicit expression for the equilibrium distance d_0 or the binding energy V_0 as a function of R. In practice, for a given radius, we minimize $V(d)$ numerically to find d_0 and V_0 at constant ρ and ε. The potential is then scaled by V_0, which amounts to choosing a reduced energy unit. Doing so enables us to compare configuration energies for different diameters.

The effective potential between two Lennard-Jones spheres shows complex but interesting variations with the distance d. At large $d \gg 2R$, the spheres are seen as pointlike and the usual 12–6 LJ interaction is recovered. At low values of $d \sim 2R+\delta$, $\delta \ll 2R$, $V(d)$ behaves as $1/\delta^7$. Typical scaled pair potentials are represented in Fig. 1 for $R = 0.1$, 0.5, 1, and 5. As R increases, the equilibrium distance d_0 gets closer to $2R$, and the potential looks much stiffer. At

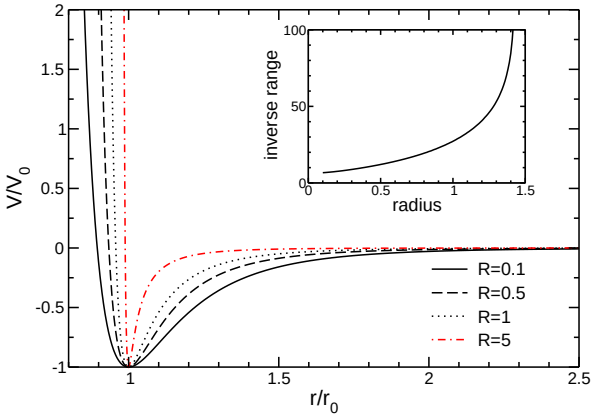

FIG. 1: Scaled pair potentials between two Lennard-Jones spheres of radius R, as a function of the reduced distance with respect to the equilibrium value. The curves corresponding to $R = 0.1$, 0.5, 1, and 5 are plotted. Inset: approximate inverse range μ of the potential versus the sphere radius.

large R, d_0 tends to $2R$ and $V_0 \to -\infty$, the interaction becomes that of infinitely attractive hard spheres. One can associate an inverse range μ to the potential by fitting it to a Morse function, $V_{\rm Morse}(d) = e^{\mu(d-d_0)}[e^{\mu(d-d_0)} - 2]$. The variations of μ versus the spheres radius are also represented in the inset of Fig. 1. For $R \to 0$, μ tends to 6, the value of the Lennard-Jones atomic potential. The range decreases monotonically with increasing R, first slowly up to $R \sim 1$, then more abruptly. The effective range is quite small ($\mu > 15$) at $R = 1$. For comparison, the Girifalco potential [14] mimicking the interaction between two buckyballs has μ close to 14 [15].

The strong variations exhibited by the effective range of the potential should have important consequences on the properties of clusters of LJ spheres. From previous work by Doye, Wales and their coworkers [16–19], significant differences in cluster structure are expected between the small and large radius regimes, or between the atomic scale and the meso scale.

III. CLOSE-PACKING TRANSITIONS

We have attempted to locate the most stable conformations of clusters of spherical particles interacting via the pair potential described in the previous section. Global optimization of cluster structure being computationally heavy, this problem has been addressed using the powerful basin-hopping algorithm of Wales and Doye [13]. Briefly, this method samples the set of isomers by performing large amplitude random displacement moves followed by a local minimization (quench). We have studied the size range $8 \leq N \leq 60$, and 5×10^4 quenches were performed for each set of size and radius. We have also borrowed the putative global minima of LJ and Morse clusters given in the Cambridge Cluster Database [20] as extra starting points for our optimizations.

We have represented in Fig. 2 some typical examples of the most stable structures found at sizes 13, 24, 29, 34 and 37 and for different values of R. These structures illustrate the three main families of clusters that were found during the global optimization process.

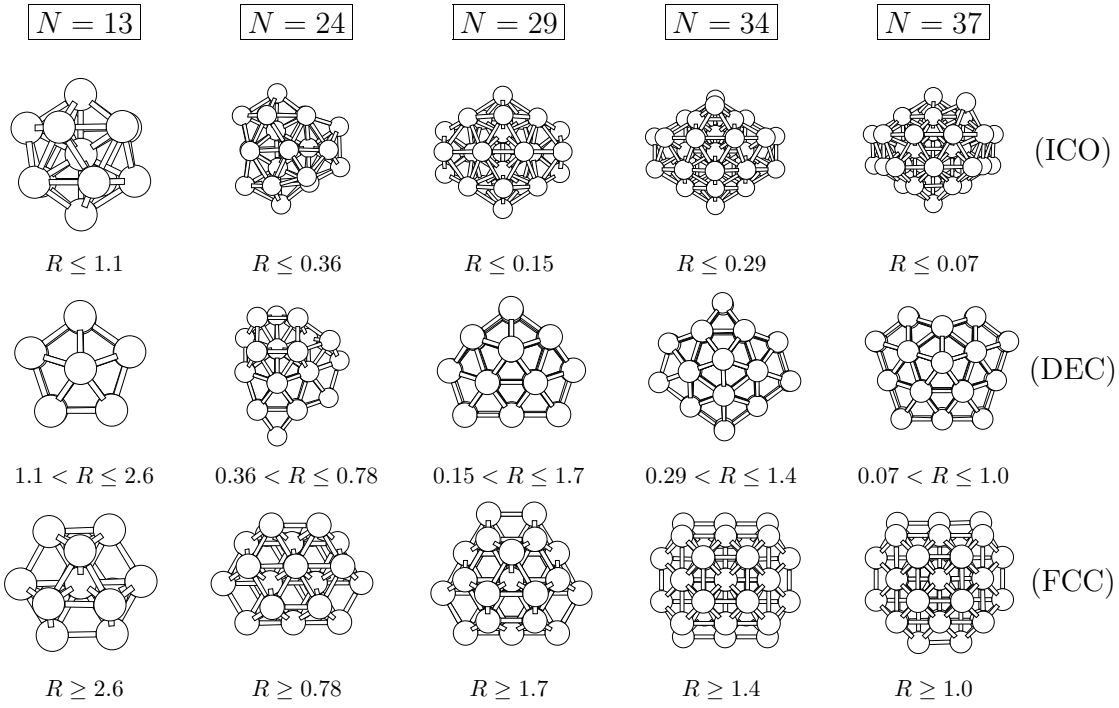

FIG. 2: Typical global minima found for $N = 13$, 24, 29, 34, and 37. All these sizes change from an icosahedral structure at low radius to a close-packed cubic structure at large radius, with an intermediate decahedral shape at medium radius.

The smallest spheres form clusters similar to atomic LJ clusters, generally with an icosahedral shape and elements of fivefold symmetry. These structures are highly coordinated, but also highly strained: most pair interactions deviate from the equilibrium distance [17]. Below $R = 1$ many global minima adopt a more compact decahedral shape, less coordinated and less strained than icosahedra. Above $R = 1$ more and more close-packed cubic structures appear. These are the fewest coordinated, but are practically free of strain.

The general phenomenology of structural transitions in clusters of LJ spheres follows that of Morse clusters [16–18], suggesting that geometry is primarily driven by the effective range of the interaction. This may not have been obvious at first sight, because the attractive interaction behaves as $1/(d - 2R)$ at low d, then as $1/d^6$ at large distances. However, the hard-core repulsion becomes nearly a contact interaction, and the potential well gets closer to the particles' diameter. Therefore, the similarity of the potential with a Morse form comes from the repulsive part, rather than from the attractive part.

The observation that cluster structure changes from icosahedral to decahedral, then to cubic seems to hold in most cases. Yet this rule has notable exceptions for sizes, which are naturally most stable in decahedral or cubic conformations in LJ atomic clusters (at $N = 75$ or 38, respectively), or when icosahedral structures are marginally stable. Fig. 3 shows the various ranges of stability of the three families of structures as a function of R, for sizes below 60 particles. Despite strong size effects, some trends are obvious on this figure. Most sizes exhibitting a two-step structural transition through an intermediate decahedral shape are indeed located near the first decahedral magic

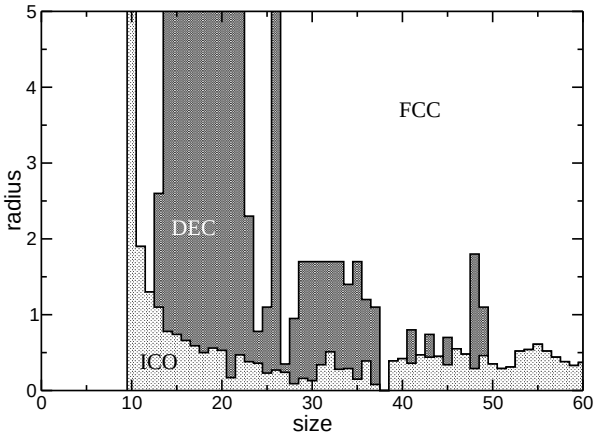

FIG. 3: Relative ranges of stability of the icosahedral (ICO), decahedral (DEC) and cubic (FCC) global minima, as a function of particle radius R and number of particles $10 \leq n \leq 60$.

number at $N = 18$, or the secondary magic number for the same series, $N = 38$. In cases near $N = 18$, the decahedral structure remains exceptionally stable even at very high values of R.

At $N = 38$ the global minimum is already close-packed at $R \to 0$, and remains so for larger particles. Only few sizes show a stable decahedral structures above this size, but we expect such geometries to be present again close to the next magic number at $N = 75$.

The critical radius where icosahedral structures are no longer the lowest in energy roughly decreases with size, and reaches about 0.7 for $N = 60$. Interestingly, the effective range is about 14 for this radius, at which clusters of C_{60} show complex structural variations [8].

It is often convenient to monitor the relative stability of clusters using the second energy difference, $D_2E(n) = E(n+1) + E(n-1) - 2E(n)$, where $E(n)$ is the cohesion energy of cluster at size n. The variations of D_2E with n are represented in Fig. 4 for the radii $R = 0.1$, 0.5, 1, and 5. Each curve $D_2E(n)$ displays peaks at the most stable sizes, but these magic numbers change with R. At low radius, they are consistent with the primary and secondary number series characteristic of Mackay ($N = 13$, 46, 49, 55) and anti-Mackay ($N = 19, 23, 26$) icosahedra. At large R, the prominent peaks at $N = 12$, 38, 50 and 59 indicate the completion of volume or surface layers in the cubic geometry. The magic numbers are harder to interpret in terms of geometry for intermediate radius, because of the strong competition between structural types.

To a large extent, the energy differences displayed in Fig. 4 are also similar to the results obtained by Doye, Wales and Berry [17]. However, one should not conclude that the stable structures of clusters of LJ spheres are identical to that of Morse clusters with the same effective range. While this is true for the vast majority of cases, several global minima found in the present study at large radius were not reported in Morse clusters, to the best of our knowledge. For instance, the close-packed structure obtained for $N = 34$ is slightly lower in energy than those reported in the Cambridge Cluster Database [20]. The interaction between large spheres has a very short range, hence the number of different minima on the PES is expected to be huge for clusters [21]. Because this interaction is not rigorously of the Morse form, there may well be small differences in the ordering between the isomers, especially at nonmagic sizes.

Finally, we have studied the large sizes regime, by restricting ourselves to the complete shell magic numbers of the icosahedral, decahedral, and cubic families. Such a coarse-grained approximation has been often used in the past to estimate crossover sizes for the appearance of bulk features in atomic clusters [3]. It has also recently been extended to include temperature [23], pressure [24] and quantum delocalization [22] effects. In the present work, a series of magic number structures are optimized at fixed R, and their energies are fitted as an expansion in $n^{-1/3}$:

$$E(n,R)/n = \alpha(R) + \beta(R)n^{-1/3} + \gamma(R)n^{-2/3} + \delta(R)n^{-1}. \tag{5}$$

The four terms in the above expansion can be seen as representing the contributions of volume, surface, edge, and vertex atoms, respectively. From the values of $(\alpha, \beta, \gamma, \delta)$ for two different structural families the relative stabilities and the possible crossover sizes can be determined. Here we have optimized clusters containing up to about 10^4 particles. In general, and in agreement with the results known on atomic LJ clusters [22], the icosahedral structure are most stable at small sizes, cubic structures are optimal at larges sizes, decahedral shapes being of intermediate stability.

The variations of the crossover sizes with increasing radius are represented in Fig. 5 as a (radius, size) phase diagram. At $R = 0.1$, the ICO→DEC→FCC transitions occur at large sizes, namely n^*(ICO→DEC) $\simeq$ 1400 and

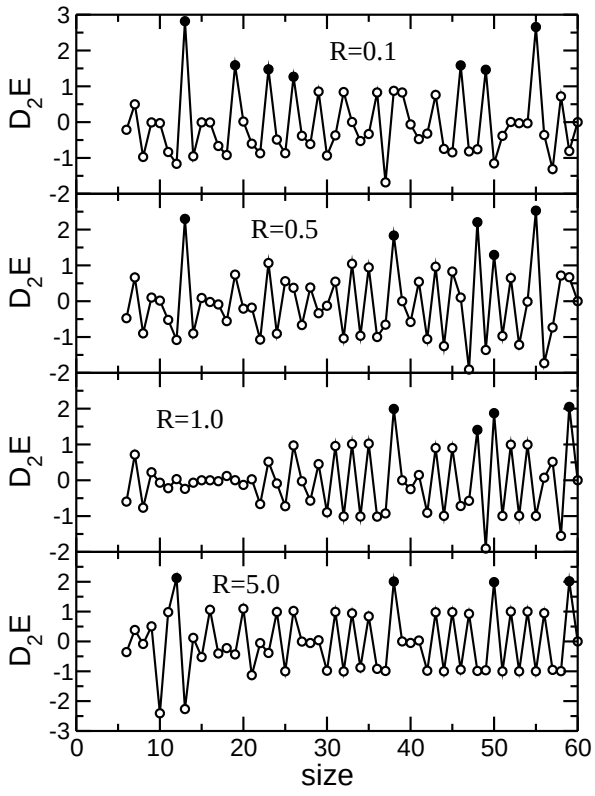

FIG. 4: Second energy differences D_2E as a function of size, for different particle radii (from top to bottom) $R = 0.1$, 0.5, 1, 5. The energies are scaled with respect to the binding energy V_0 of the dimer at equilibrium, and particularly stable sizes (magic numbers) are emphasized as solid dots.

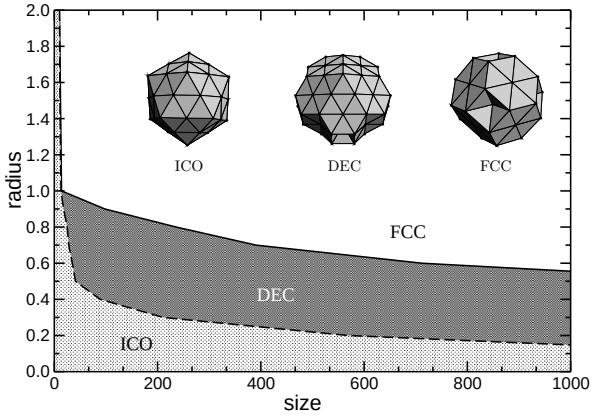

FIG. 5: Relative stabilities of the icosahedral (ICO), decahedral (DEC) and close-packed cubic (FCC) structures of large clusters of LJ spherical particles as a function of size, for increasing particle radius.

n^*(DEC→FCC) $\simeq$ 10000. These values are rather close to the crossover sizes in LJ atomic clusters [22]. Icosahedral shapes become rapidly less stable at intermediate or large R: already at $R = 0.4$, the two-layer Mackay icosahedron ($n = 55$) is no longer the most stable, in rough agreement with the more detailed picture of Fig. 3. Eventually, above $R = 1$, only the cubic structures are significantly lower in energy than the two other families.

The above results are consistent with our previous findings on smaller clusters, and tell us that clusters of LJ spheres behave mostly as hard spheres as soon as $R \gtrsim 1$. The close-packing scheme adopted by these particles significantly enriches the energy landscape of the clusters [19]. From a numerical point of view, it should also simplify the optimization procedure, because only geometries based on the cubic ordering could be sampled. In this respect,

lattice-based searches should be used preferentially.

IV. SUMMARY AND CONCLUSIONS

The stable structures of clusters of spherical particles bound by elementary Lennard-Jones forces have been investigated in the small and large sizes regimes. Assuming that the particles were homogeneously filled, the exact pair interaction was calculated as a function of the radius R and the distance d between the centers of mass. The pair potential was scaled and reduced units were used to allow for a comparison upon changing R.

As the radius is increased, we generally find that clusters become more and more compact, exhibiting first icosahedral, then decahedral, and finally close-packed cubic shapes. Finite-size effects remain rather strong in the size range $n \leq 60$, as the onset of the close-packed character appears at different radius depending on n. The possible occurence of magic numbers corresponding to the different packing schemes is another complicating factor. Larger clusters were seen to favor also cubic structures as soon as the radius exceeds the LJ atomic distance σ.

Most of the present results could be interpreted from the effective range of the pair interaction, which decreases very sharply with increasing R, as well as from the numerous data on Morse clusters. These similarities suggest that the thermodynamical [25, 26] and dynamical [27] properties of the present aggregates and their bulk forms will also show intriguing properties.

At least two extensions of the present work are anticipated. Heterogeneous clusters offer a much more challenging test for global optimization, for which designated algorithms have recently been developed [28]. Clusters of particles with two or more kinds of diameters should show a far richer structural diagram than homogeneous systems, even possibly different from the typical geometries reported here. Another extension would be to account for temperature effects. However, the divergence of the binding energy with increasing radius will require giving up the power law repulsive part. A softer exponential function should provide a more realistic description of the short-range Pauli repulsion between the particles.

[1] R. L. Johnston *Atomic and Molecular Clusters* (Taylor & Francis, London, 2002).
[2] B. Hartke, Angew. Chem. **41**, 1468 (2002).
[3] F. Baletto and R. Ferrando, Rev. Mod. Phys. **77**, 371 (2005).
[4] B. Raoult, J. Farges, M.-F. de Feraudy, and G. Torchet, Philos. Mag. B **60**, 881 (1989).
[5] T. P. Martin, T. Bergmann, H. Göhlich, and T. Lange, Chem. Phys. Lett. **172**, 209 (1990).
[6] F. Calvo, G. Torchet, and M.-F. de Feraudy, J. Chem. Phys. **111**, 4650 (1999).
[7] J.-B. Maillet, A. Boutin, and A. H. Fuchs, J. Chem. Phys. **111**, 2095 (1999).
[8] J. P. K. Doye, D. J. Wales, W. Branz, and F. Calvo, Phys. Rev. B **64**, 235409 (2001).
[9] F. Calvo and F. Spiegelman, Phys. Rev. B **54**, 10949 (1996).
[10] D. Y. Sun and X. G. Gong, Phys. Rev. B **54**, 17051 (1996).
[11] H. C. Hamaker, Physica **10**, 1058 (1937).
[12] F. H. Stillinger, Phys. Rev. E **59**, 48 (1999).
[13] D. J. Wales and J. P. K. Doye, J. Phys. Chem. A **101**, 5111 (1997).
[14] L. A. Girifalco, J. Phys. Chem. **96**, 858 (1992).
[15] D. J. Wales and J. Uppenbrick, Phys. Rev. B **50**, 12342 (1994).
[16] P. A. Braier, R. S. Berry, and D. J. Wales, J. Chem. Phys. **93**, 8745 (1990).
[17] J. P. K. Doye, D. J. Wales, and R. S. Berry, J. Chem. Phys. **103**, 4234 (1995).
[18] J. P. K. Doye and D. J. Wales, J. Chem. Soc., Faraday Trans. **93**, 4233 (1997).
[19] M. A. Miller and D. J. Wales, J. Chem. Phys. **111**, 6610 (1999).
[20] The Cambridge Cluster Database, `http://www-wales.ch.cam.ac.uk:/CCD.html`
[21] D. J. Wales, *Energy Landscapes*, Cambridge University, Cambridge, 2003.
[22] J. P. K. Doye and F. Calvo, J. Chem. Phys. **116**, 8307 (2002).
[23] J. P. K. Doye and F. Calvo, Phys. Rev. Lett. **86**, 3570 (2001).
[24] F. Calvo and J. P. K. Doye, Phys. Rev. B **69**, 125414 (2004).
[25] C. Rey, J. Garcína-Rodeja, L. J. Gallego, and M. J. Grimson, Phys. Rev. E **57**, 4420 (1998).
[26] M. Moseler and J. Nordiek, Phys. Rev. B **60**, 11734 (1999).
[27] J. P. K. Doye and D. J. Wales, J. Phys. B **29**, 4859 (1996).
[28] F. Calvo and E. Yurtsever, Phys. Rev. B **70**, 045423 (2004).